J. Nonlinear Var. Anal. 6 (2022), No. 2, pp. 113-124
Available online at http://jnva.biemdas.com
https://doi.org/10.23952/jnva.6.2022.2.08

DYNAMIC OPTIMIZATION WITH A NON-SMOOTH LPV SYSTEM IN AERO-ENGINE TRANSITION STATE ACCELERATION PROCESS

JIAO TENG[1,4], KE GUO[2,*], LEI WANG[1,3]

[1]*School of Mathematical Sciences, Dalian University of Technology, Dalian, China*
[2]*School of Mathematics and Information, China West Normal University, Nanchong, China*
[3]*School of Science, Department of Mathematics, Shihezi University, Shihezi, Xinjiang, China*
[4]*Key Laboratory of Intelligent Control and Optimization for Industrial Equipment, Dalian University of Technology, Dalian, China*

Abstract. In this paper, we study the dynamic optimization of the acceleration process in the engine transition state. It is difficult for general linear and nonlinear models to portray the complex mechanical characteristics of an aero-engine. We consider a non-smooth linear parameter variation (LPV) system with nonlinear terms as a mathematical model for this acceleration process. First, a control parameterization method is used to transform the problem into a parameter selection problem. Then, a smoothing technique is used to deal with the non-smooth state constraints. Finally, in order to obtain the global optimal solution of this dynamic optimization problem, an optimization algorithm based on a combination of a gradient descent method and a modified particle swarm optimization is designed to solve the equivalent nonlinear programming problem. The effectiveness and superiority of the proposed algorithm is computationally verified by using the LPV model identified from the actual data.

Keywords. Control parameterization; Dynamic optimization; LPV system; Particle swarm optimization.

1. Introduction

The aero-engine powers the aircraft flight, and its performance will directly affect the reliability of the aircraft. With the progress of aero-space technology, the aero-engine is developing towards high mobility and intelligence, and the dynamic optimization problem in the background of aero-engine is receiving more and more attention; see, e.g., [1,2]. In different phases of flight, the vehicle has different requirements for the engine thrust. The process of switching from one working state to another is known as the transition process, and the transition state regulator plays a key role in the aero-engine control system, accounting for about 75% of the whole control design cycle [3]. The complex dynamic properties of aero-engines determine that simple linear systems cannot achieve an accurate description of an aero-engine. Although nonlinear functions can capture more characteristics of an engine system, most of the controller

*Corresponding author.
E-mail addresses: jtengmath@163.com (J. Teng), keguo2014@126.com (K. Guo), wanglei@dlut.edu.cn (L. Wang).

Received November 1, 2021; Accepted January 20, 2022.

design methods cannot be directly applied to nonlinear systems. The linear variable parameter systems build a bridge between linear and nonlinear systems, allowing the applications of results from the well-established linear system theory to nonlinear systems [4, 5].

In the 1990s, Shamma first proposed the expanded LPV control based on the LPV model, a special structural system that solves the stability and smooth transition problems of traditional gain scheduling control. LPV systems have been studied in many engineering fields. In [6], the applications of a discrete LPV concept for freeway traffic modeling and identification were presented. In [7], the LPV control design techniques were applied to the problem of slip control for two-wheeled vehicles. In [8], an LPV gain scheduled control strategy was proposed to regulate the oxygen stoichiometry of the PEMFC. Without coincidence, LPV control has also been widely applied in the field of aero-engine control [9–12]. In [11], based on a kind of linearization model, the switch LPV aero-engine model was established and the tracking control law was designed to obtain the ideal H_∞ tracking performance. In [12], the problem of H_∞ output tracking control for a class of switched LPV systems via multiple parameter-dependent Lyapunov functions was studied. Compared with existing dynamic optimization problems, the dynamic optimization problem studied in this paper is characterized by the LPV system itself. Although the switching moments are fixed, the arrangement of the switching subsystems depends entirely on the scheduling parameters at each sampling time, and the system is nonsmooth at the switching point. Moreover, the set of switching subsystems is still essentially infinite-dimensional. Therefore, it is more difficult to use conventional gradient-based methods directly, which also bring the complexity to theoretical analysis, numerical simulation, and computation. In recent years, many theoretical or practical researches on the dynamic optimization problem [13–15] were performed. Moreover, due to the complexity of aero-engine systems, it is difficult to give expressions of analytical solutions in the form of [16, 17] by using methods, such as Pontryagin's extreme value principle or Bellman's dynamic programming. As a heuristic algorithm, the particle swarm optimization (PSO) algorithm can avoid solving gradient information, which is difficult to obtain. PSO algorithm has the characteristic that it can jump out of the local optimal solutions. As an important branch of evolutionary algorithm, particle swarm optimization algorithm has the advantages of easy implementation, high efficiency, and strong nonlinear optimization performance, and has been widely used in many fields; see, e.g., [18, 19]. In this paper, we study the acceleration process in the transition state of the aero-engine. In the process of engine operation, on the one hand, it is necessary to ensure the safe operation of the engine, and on the other hand, it is critical to run the engine as close to the limit as possible so that performance can be fully realized. So, we add constraints on the state variables and control variables to the dynamic optimization problem. After translating the problem using control parameterization and smoothing techniques, we use a numerical computational method based on the modified particle swarm optimization (MPSO) algorithm combined with the gradient descent method to calculate the solution.

The innovations of our work are summarized below. (1) the LPV system is nonsmooth at each switching point; (2) the smoothing technique is required before obtaining the gradient information of the state constraint function with respect to the control variables; (3) the infinite-dimensional dynamic optimization problem can be transformed into a finite-dimensional optimal parameter selection problem by the control parameterization method; and (4) the proposed improved particle swarm algorithm can effectively reduce the oscillation of the fuel control and speed output. The remainder of this paper is organized as follows. In Section 2, the non-smooth LPV model is described. In Section 3, we propose the dynamic optimization problem based on aero-engine transition state accelerated process. Section 4 and Section 5 propose a method to solve the dynamic optimization problem based on control parameterization and the MPSO algorithm. Section 6 illustrates the numerical results. Finally, the conclusions are provided in Section 7, the last section.

2. Non-smooth LPV Systems Description

Aero-engine system is a complex non-linear system. Designing engine controllers via a non-linear system model can ensure high accuracy, but comes with a large number of calculations. So, there are few practical applications in engineering. LPV systems can well describe non-linear the systems with a wide range of dynamic characteristic variations, and the nonlinearity of LPV systems can be hidden in the variable parameters so that the control system with satisfactory accuracy can be designed using linear theory. By identifying the dynamic models of the aero-engine at different steady states and combining the corresponding steady-state models with polynomial fitting and least-squares support vector machines, the transition process of the aero-engine can be characterized as the following non-smooth model:

$$\begin{aligned} \dot{x}(t) &= \begin{bmatrix} a_{11}(\rho_k) & a_{12}(\rho_k) \\ a_{21}(\rho_k) & a_{22}(\rho_k) \end{bmatrix} x(t) + \begin{bmatrix} b_1(\rho_k) \\ b_2(\rho_k) \end{bmatrix} (u(t) - \varphi(\rho_k)), \\ y(t) &= [c_1(\rho_k) \quad c_2(\rho_k)]\, x(t) + \psi(u(t)), \\ t &\in I_k, k = 1, 2, \ldots, m, \end{aligned} \tag{2.1}$$

where I_k is sampling interval and denoted as: $I_k := [(k-1)T, kT)$, $k = 1, \ldots, m$, the initial time $t_0 := 0$, the given termination time $t_f := mT$, m represents the number of time intervals, and kT, $k = 1, 2, \ldots, m$ are the switching time series with time interval length T being given.

The scheduling parameter ρ_k can be mathematically expressed as:

$$\rho_k = y((k-1)T), k = 1, \ldots, m. \tag{2.2}$$

where $x(t)$ represents the relative transition speed state value of the high and low pressure turbine during the transition of the aero-engine, $u(t) \in \mathbb{R}^{n_u}$ denotes the control variable at time t, which represents the oil quantity signal input during the aero-engine transition process, and $y(t)$ represents the relative conversion speed output of the high-pressure turbine during the aero-engine transition. $\psi(.), \phi(.)$ can be obtained by a higher order polynomial fitting method, $a_{11}(\cdot)$, $a_{12}(\cdot)$, $a_{21}(\cdot)$, $a_{22}(\cdot)$, $b_1(\cdot)$, $b_2(\cdot)$, $c_1(\cdot)$, and $c_2(\cdot)$ are usually given as a non-linear function of ρ or $u(t)$.

3. Dynamic Optimization Problem

The purpose of this section is to give the corresponding dynamic optimization problem for the aero-engine transition state acceleration optimization process with various constraints in actual operation. The choice of the objective function is very important in the acceleration problem of an aero-engine. It is related to the acceleration performance of the engine. The goal of engine acceleration process optimization is to make the actual engine rotor speed reach the set steady-state speed more quickly in a certain period of time and to keep track of the steady-state speed. The rapid increase of thrust is important in the actual operation of the engine, however, it is not easy to measure the thrust directly, and the magnitude of the thrust is usually reflected by the rate of increase in engine speed. Therefore, we describe the objective function for the optimization of the engine acceleration process by the following equation

$$J = \int_0^{t_f} [y(t) - y_{obj}]^2 dt, \tag{3.1}$$

where $y(t)$ is the actual speed output, y_{obj} is the objective speed, and t_f is the given termination time.

According to the actual engine operation process, the oil quantity input needs to vary within a definite range based on the consideration of the safety and effectiveness of engine operation, so do the relative transition speed state value of the high and low pressure turbine. Therefore the following constraints on the control and state variables need to be considered, i,e,

$$u(t) \in U \triangleq [u_*, u^*] \subset \mathbb{R}_+, \tag{3.2}$$

$$x(t|u) \in W \triangleq \prod_{j=1}^{2} \left[x_{j*}, x_j^*\right] \subset \mathbb{R}_+^2, \quad \forall t \in I, \tag{3.3}$$

where u_* and u^*, x_{j*} and $x_j^*, j = 1,2$ are the given real number, and satisfy $u_* < u^*, x_{1*} < x_1^*, x_{2*} < x_2^*$. Any Borel measurable function $u : [t_0, t_f] \to R^{n_u}$ satisfying (3.2) and (3.3) almost everywhere is called an admissible control. Let $\mathscr{U}$ denote the class of all such admissible controls.

The dynamic optimization problem of the acceleration process in the transition state is as follows.

Problem 3.1.

$$\begin{aligned}
(\text{OCP}) : \min \quad & J = \int_0^{t_f} \left[y(t) - y_{obj}\right]^2 dt \\
s.t.\ \dot{x}(t) &= \begin{bmatrix} a_{11}(\rho_k) & a_{12}(\rho_k) \\ a_{21}(\rho_k) & a_{22}(\rho_k) \end{bmatrix} x(t) + \begin{bmatrix} b_1(\rho_k) \\ b_2(\rho_k) \end{bmatrix} (u(t) - \varphi(\rho_k)), \\
y(t) &= [c_1(\rho_k) \quad c_2(\rho_k)]\, x(t) + \psi(u(t)), \\
\rho_k &= y((k-1)T), k = 1, \ldots, m, \\
u(t) &\in U, x(t|u) \in W.
\end{aligned} \tag{3.4}$$

4. COMPUTATIONAL APPROACHES

4.1. **Problem transformation based on control parameterization.** It is really challenging to obtain analytical solutions to dynamic optimization in complex real-world problems. Therefore, we consider the applications of a control parameterization method to obtain numerical solutions, which approximate the optimal control by a linear combination of a series of basis functions so that the infinite-dimensional control problem can be transformed into an optimization problem with finite optimization variables [20, 21].

With piecewise-constant basis functions, the control signal u is approximated as follows:

$$u(t) \approx u^p(t) = \xi^k, \quad t \in [\tau_{k-1}, \tau_k), \quad k = 1, \ldots, p, \tag{4.1}$$

where $p \geq 1$ is the number of control subintervals, $[\tau_{k-1}, \tau_k)$ is the kth control subinterval, and ξ^k is the value of the control on the kth subinterval. The constant control values $\xi^k, k = 1, \ldots, p$, are decision variables to be chosen optimally, while $\tau_k, k = 0, \ldots, p$, are pre-fixed knot points satisfying $0=\tau_0<\tau_1<\tau_2<\cdots<\tau_{p-1}<\tau_p=t_f$. The approximate piecewise-constant control can be written as follows: $u^p(t|\xi):=\sum_{k=1}^{p}\xi^k\chi_{[\tau_{k-1},\tau_k)}(t)$, $t\in[0,t_f]$, where $\xi=\left[\xi^1,\ldots,\xi^p\right]^\top\in R^p$, and $\chi_{[\tau_{k-1},\tau_k)}:R\to R$ is the characteristic function defined by

$$\chi_{[\tau_{k-1},\tau_k)}(t):=\begin{cases}1, & \text{if } t\in[\tau_{k-1},\tau_k),\\ 0, & \text{if } t\notin[\tau_{k-1},\tau_k).\end{cases}$$

Substituting (4.1) into the dynamic system yields,

$$\begin{cases}\dot{x}(t)=f^k\left(x(t),\rho_k,\xi^k\right),\\ y(t)=C(\rho_k)x(t)+\psi\left(\xi^k\right),\\ x(t_0)=x_0.\end{cases}\tag{4.2}$$

in which $f^k\left(x(t),\rho_k,\xi^k\right):=A(\rho_k)x(t)+B(\rho_k)(\xi^k-\phi(\rho_k))$. Substituting (4.1) into the cost function (3.1) yields,

$$J=\sum_{k=1}^{p}\int_{(k-1)T}^{kT}[y^k(t)-y_{obj}]^2dt.\tag{4.3}$$

Remark 4.1. p represents the number of segments of the control parameterization, and m represents the number of sampling periods of the LPV system. In the actual calculation process, we can flexibly adjust p to be an integer multiple of m. Therefore, in the following discussion, to avoid ambiguity, we unify them into p.

Thus, using control parameterization (4.1), Problem 3.1 can be approximated by the following finite-dimensional optimization problem:

Problem 4.1. *With dynamic system (4.2), choose the vector $u^p(.\mid\xi)\in\mathscr{U}$ such that the cost function (4.3) is minimized.*

4.2. **Handling of state constraints.** For Problem 4.1, it is not easy to directly determine whether the constraints (3.3) on state variables hold or not. To overcome this challenge, we perform a series of transformations to the constraints, introducing new constraint functions and presenting the corresponding gradient information.

First, substituting (4.1) into the cost function (3.3) yields

$$x^k(t|\xi^k)\in W\triangleq\prod_{j=1}^{2}\left[x_{j*},x_j^*\right]\subset\mathbb{R}_+^2,\quad\forall t\in I,k=1,\ldots,p.$$

Let

$$g_j^k(x(t|\sigma^k)):=x_j^k(t|\sigma^k)-x_j^*,g_{2+j}^k(x(t|\sigma^k)):=x_{j*}-x_j^k(t|\sigma^k),j\in I_2,k=1,\ldots,m.$$

Constraint (3.3) can be equivalently transcribed into:

$$G^k(\xi^k)=0,\tag{4.4}$$

where

$$G^k(\xi^k):=\sum_{j=1}^{4}\int_{(k-1)T}^{kT}\max\left\{0,g_j^k(x(t|\xi^k))\right\}\mathrm{d}t.$$

However, $G^k(\xi^k)$ is non-smooth so we replace (4.4) with

$$G_\varepsilon^k(\xi^k) := \sum_{j=1}^{4} \int_{(k-1)T}^{kT} \varphi_{\varepsilon,j}^k(t|\xi^k)dt \leq 0, \tag{4.5}$$

where $\varepsilon > 0$ and

$$\varphi_{\varepsilon,j}^k(x(t|\sigma^k)) := \begin{cases} 0, & g_j^k(x(t|\sigma^k)) < -\varepsilon, \\ \frac{\left(g_j^k(x(t|\sigma^k))+\varepsilon\right)^2}{4\varepsilon}, & -\varepsilon \leq g_j^k(x(t|\sigma^k)) \leq \varepsilon, \\ g_j^k(x(t|\sigma^k)), & g_j^k(x(t|\sigma^k)) > \varepsilon. \end{cases}$$

Next, we give the gradient information of the constraint function (4.5) with respect to the control. First, for each $k = 1,\ldots,p$, we consider the following auxiliary dynamic system:

$$\dot{\psi}_i^k(t) = \hat{\rho}_{k,l} \frac{\partial f\left(x(t|\xi),\rho_l,\xi^l\right)}{\partial x} \cdot \psi_i^k(t) + \rho_{k,l} \frac{\partial f\left(x(t|\xi),\rho_l,\xi^l\right)}{\partial u_i}, \tag{4.6}$$

and

$$\psi_i^k(0) = 0, t \in I_k, k = 1,\ldots,p, i = 1,\ldots,r. \tag{4.7}$$

Theorem 4.1. *For each $\varepsilon > 0$, the derivatives of the constraint functionals $G_\varepsilon^k(\xi^k)$ with respect to the ith component of the parameter vector are*

$$\frac{\partial G_\varepsilon^k(\xi^k)}{\partial \xi_i^k} = \sum_{j=1}^{4} \int_{(k-1)T}^{kT} \frac{\varphi_{\varepsilon,j}^k(x(t|\xi^k))}{\partial x} \cdot \psi_i^k(t)dt,$$
$$k = 1,\ldots,p, \quad i = 1,\ldots,r.$$

Proof. Differentiating the equation (4.5) with respect to ξ_i^k yields

$$\frac{\partial G_\varepsilon^k(u)}{\partial \xi_i^k} = \sum_{j=1}^{4} \int_{(k-1)T}^{kT} \frac{\varphi_{\varepsilon,j}^k(x(t|u))}{\partial x} \cdot \frac{\partial x(s|\xi)}{\partial \xi_i^k} dt, \quad k = 1,\ldots,p, i = 1,\ldots,r. \tag{4.8}$$

As $x(t|u)$ is the solution to dynamic system (4.2), we have

$$x(s|\xi) = x(\alpha_{l-1}|\xi) + \int_{\alpha_{l-1}}^{s} f\left(x(\eta|\xi),\rho_l,\xi^l\right) d\eta, s \in I_l. \tag{4.9}$$

If $l > k$, then we differentiate (4.9) with respect to ξ_i^k to obtain

$$\frac{\partial x(s|\xi)}{\partial \xi_i^k} = \frac{\partial x(\alpha_{l-1}|\xi)}{\partial \xi_i^k} + \int_{\alpha_{l-1}}^{s} \frac{\partial f\left(x(\eta|\xi),\rho_l,\xi^l\right)}{\partial x} \cdot \frac{\partial x}{\partial \xi_i^k} d\eta. \tag{4.10}$$

If $l = k$, then

$$\frac{\partial x(s|\xi)}{\partial \xi_i^k} = \frac{\partial x(\alpha_{l-1}|\xi)}{\partial \xi_i^k} + \int_{\alpha_{l-1}}^{s} \frac{\partial f\left(x(\eta|\xi),\rho_l,\xi^l\right)}{\partial x} \cdot \frac{\partial x}{\partial \xi_i^k} d\eta + \int_{\alpha_{l-1}}^{s} \frac{\partial f\left(x(\eta|\xi),\rho_l,\xi^l\right)}{\partial u_i} d\eta. \tag{4.11}$$

If $l < k$, then

$$\frac{\partial x(s|\xi)}{\partial \xi_i^k} = 0. \tag{4.12}$$

Combining equations (4.10)-(4.12) gives,

$$\begin{aligned}\frac{\partial x(s|\xi)}{\partial \xi_i^k} =&\hat{\rho}_{k,l}\left[\frac{\partial x(\alpha_{l-1})}{\partial \xi_i^k}+\int_{\alpha_{i-1}}^{s}\frac{\partial f\left(x(\eta|\xi),\rho_l,\xi^l\right)}{\partial x}\cdot\frac{\partial x}{\partial \xi_i^k}d\eta\right]\\ &+\int_{\alpha_{l-1}}^{s}\rho_{k,l}\frac{\partial f\left(x(\eta|\xi),\rho_l,\xi^l\right)}{\partial u_i}d\eta, s\in J_l.\end{aligned} \tag{4.13}$$

By differentiating this equation with respect to s, we arrive at

$$\begin{aligned}\frac{d}{ds}\left\{\frac{\partial x(s|\xi)}{\partial \xi_i^k}\right\} = \hat{\rho}_{k,l}\frac{\partial f\left(x(s|\xi),\rho_l,\xi^l\right)}{\partial x}\cdot\frac{\partial x}{\partial \xi_i^k}+\rho_{k,l}\frac{\partial f\left(x(s|\xi),\rho_l,\xi^l\right)}{\partial u_i},\\ s\in J_l, l=1,\ldots,p.\end{aligned} \tag{4.14}$$

Moreover,

$$\frac{\partial x(0|\xi)}{\partial \xi_i^k}=0, \tag{4.15}$$

where

$$\rho_{k,l}=\begin{cases}1, \text{ if } k=l,\\ 0, \text{ otherwise,}\end{cases}$$

and

$$\hat{\rho}_{k,l}=\begin{cases}1, & \text{if } k\le l,\\ 0, & \text{otherwise.}\end{cases}$$

Equations (4.14)-(4.15) show that $\frac{\partial x(s|\xi)}{\partial \xi_i^k}$ is a solution to (4.6)-(4.7). By the theory of differential equations [22], we see that such a solution is unique. Therefore,

$$\frac{\partial x(t|\xi)}{\partial \xi_i^k}=\psi_i^k(t).$$

Substituting this equation into (4.8) completes the proof. □

5. Numerical Algorithms Based on Particle Swarm Optimization

In the traditional optimization algorithm, the gradient of the optimization function needs to be used to solve the optimization problem, which puts forward higher requirements for the mathematical properties of the function to be optimized, while the intelligent optimization algorithm does not need gradient information, which greatly reduces the requirements of the objective function to be optimized. Particle swarm optimization (PSO) algorithm was first mentioned by Kennedy and Eberhart [23] in 1995. This algorithm has the advantages of simple optimization principle, fewer calculation parameters, parallel search, and global convergence. On the basis of classical particle swarm optimization, we use an improved particle swarm optimization algorithm (MPSO) to solve the dynamic optimization problem. In the actual operation of the engine, the fuel quantity controlled at the previous time will affect the next time, and the control value of the previous time is added to the formula with a certain weight when updating the particle position. The velocities and positions of the particles in the MPSO algorithm are updated as follows:

- The positions of the qth particle in the $I_{ter}th$ iteration are:
  $u_q^{I_{ter}}=\left(u_{q1}^{I_{ter}},u_{q2}^{I_{ter}},\ldots,u_{qp}^{I_{ter}}\right), u_{qp}^{I_{ter}}\in[u_{lb},u_{ub}]$,

- The velocities of the qth particle in the $I_{ter}th$ iteration are:
$v_q^{I_{ter}} = \left(v_{q1}^{I_{ter}}, v_{q2}^{I_{ter}}, \ldots, v_{qp}^{I_{ter}}\right), v_{qp}^{I_{ter}} \in [v_{min}, v_{max}]$,
- J^* is the optimal objective function value of the whole group,
- $J^{I_{ter}*}$ represents the value of J^* at the end of the $I_{ter}th$ iteration.

During the optimization process, the following variables are required

$$v_q^{I_{ter}+1} = w(q)v_q^{I_{ter}} + c_1 l_1 \left(p_q^{I_{ter}} - u_q^{I_{ter}}\right) + c_2 l_2 \left(g^{I_{ter}} - u_q^{I_{ter}}\right), \tag{5.1}$$

and

$$u_{q,p}^{I_{ter}+1} = \alpha * u_{q,p-1}^{I_{ter}} + (1-\alpha) * u_{q,p}^{I_{ter}} + v_q^{I_{ter}+1}, \alpha \in (0,1). \tag{5.2}$$

where, the constraint factor of speed is:

$$w(q) = 0.4 + 0.5 * exp(-3 * (I_{ter}/I_{max})^2),$$

where, $v_q^{I_{ter}}$ and $u_q^{I_{ter}}$ are velocity and position of the qth particle in the $I_{ter}th$ iteration, respectively, $p_q^{I_{ter}}$ is the best position of the qth particle in the previous $I_{ter}th$ iteration, $g^{I_{ter}}$ is the best place in the $I_{ter}th$ iteration group, and $I_{\max}$ is the maximum number of iterations. Based on the above calculation of the gradient information about the state constraints on the control variables, we combine the gradient descent algorithm and the MPSO to give the following algorithm for solving the problem 4.1:

Algorithm 5.1. ***Step 1*** *Set constants* $c_1, c_2 > 0$ *and random numbers* $l_1, l_2 \in [0, 1]$*;*

Step 2 *Generate* Q *initial particles with a uniform distribution on* U *randomly. Denote the position and velocity of particles by* $u_q^{I_{ter}} \in U$ *and* $v_q^{I_{ter}} \in V := [v_{\min}, v_{\max}]$*, respectively, and calculate* $J_q^{I_{ter}*}$*;*

Step 3 *For each particle* $u_q^{I_{ter}}$*, obtain* $\rho_k, i = 2, \ldots, p$ *by solving dynamic system (2.1) and the equation (2.2), and calculate the cost function* $J_q^{I_{ter}}$*;*

Step 4 *Check the value of* $G_{\varepsilon,\gamma}\left(u_q^{I_{ter}}\right)$*. If* $G_{\varepsilon,\gamma}\left(u_q^{I_{ter}}\right) \leq 0$*, then compute* $J\left(u_q^{I_{ter}}\right)$*, and set* $q = q+1$*; otherwise, move the parameter towards the feasible region in the negative direction of* $\frac{\partial G_{\varepsilon,\gamma}\left(u_q^{I_{ter}}\right)}{\partial u_q^{I_{ter}}}$ *until* $G_{\varepsilon,\gamma}\left(u^{I_{ter},j}\right) \leq 0$*;*

Step 5 *For each particle, update the historical optimal objective function value* $J_q^{I_{ter}*}$*. If* $J_q^{I_{ter}} > J_q^{I_{ter}-1}$*, then* $J_q^{I_{ter}*} = J_q^{I_{ter}}$*, otherwise,* $J_q^{I_{ter}*} = J_q^{I_{ter}-1*}$*;*

Step 6 *Compute and save* $J_*^{I_{ter}} = \max_{q=1,2,\ldots Q} J_{q*}^{I_{ter}}$*, and* $u_*^{I_{ter}} = \arg\max_{q=1,2,\ldots Q} J_{q*}^{I_{ter}}$*;*

Step 7 *Update the velocity and position of the particle* $v_q^{I_{ter}}$ *and* $u_q^{I_{ter}}$ *according to equation (5.1) and (5.2);*

Step 8 *If* $I_{ter} > I_{\max}$ *or* $J_*^{I_{ter}} - J_*^{I_{ter}-1} < \eta$*, then end the iteration; otherwise, set* $I_{ter} = I_{ter} + 1$ *and go to Step 3.*

Remark 5.1. Let σ denote the solution of the approximate Problem 4.1, and let u^* denote the solution of the classic dynamic optimization problem 3.1. Under suitable conditions, based on [24–26], we can similarly obtain the following convergent result

$$\lim_{p\to\infty} J\left(u\left(\cdot|\sigma^{p,*}\right)\right) = J\left(u^*\right).$$

6. Numerical Results

In this section, we use the model identified from the actual data for numerical calculation. The model identification process is as follows: the excitation signals (e.g., random Gaussian signals, binary signals, or sinusoidal signals) constructed by MATALB's IDINPUT command are input to the nonlinear engine model to obtain the output data, and then the corresponding set of input and output data is imported into the MATALB System Identification Toolbox for model identification. The polynomial expression is obtained by fitting the data of 23 operating points by using the linear state space model of the identified 23 operating points.

Based on the LPV system (3.4), we set $y_{obj} = 100$. The dynamic optimization problem is described as follows:

$$\begin{aligned}
&\min \quad J = \int_0^{t_f} [y(t) - y_{obj}]^2 dt \\
&\dot{x}(t) = \begin{bmatrix} a_{11}(\rho_k) & a_{12}(\rho_k) \\ a_{21}(\rho_k) & a_{22}(\rho_k) \end{bmatrix} x(t) + \begin{bmatrix} b_1(\rho_k) \\ b_2(\rho_k) \end{bmatrix} (u(t) - \varphi(\rho_k)), \\
&y(t) = [c_1(\rho_k) \quad c_2(\rho_k)]\, x(t) + \psi(u(t)), \\
&\rho_k = y((k-1)T), k = 1, \ldots, 321.
\end{aligned} \tag{6.1}$$

where $x(t) \in R^2$ is state variable, $y(t) \in R$ is observed quantity, $u(t) \in R$ is control variable, and $\rho_k \in R$ is time-varying parameter.

The coefficient matrix are shown as follows

$$\begin{aligned}
&a_{11}(\rho_k) = -0.0009111 * \rho_k^2 + 0.1211 * \rho_k - 4.182, \\
&a_{12}(\rho_k) = (2.665e-05) * \rho_k^2 - 0.07154 * \rho_k + 4.182, \\
&a_{21}(\rho_k) = 0.003114 * \rho_k^2 - 0.3054 * \rho_k + 22.71, \\
&a_{22}(\rho_k) = -27.87 - 9.256 * \cos(0.1291 * \rho_k) + 8.106 * \sin(0.1291 * \rho_k) \\
&\qquad\qquad -2.007 * \cos(2 * 0.1291 * \rho_k) - 4.322 * \sin(2 * 0.1291 * \rho_k), \\
&b_1(\rho_k) = 0.004927 * \rho_k - 0.3658, \\
&b_2(\rho_k) = (2.069e-05) * \rho_k^2 - 0.04307 * \rho_k - 0.3973, \\
&c_1(\rho_k) = 0.001185 * \rho_k^2 - 0.2396 * \rho_k + 12.31, \\
&c_2(\rho_k) = (-5.059e-06) * \rho_k^2 + 0.001153 * \rho_k - 0.06741, \\
&\varphi(\rho_k) = 0.4206 * \rho_k^2 - 62.94 * \rho_k + 2427, \\
&\psi(u) = 9.196e-07 * u^3 - 0.000782 * u^3 + 0.2706 * u + 62.29.
\end{aligned} \tag{6.2}$$

Based on actual data, we set $u_* = 80, u^* = 360, x_{1*} = 52, x_1^* = 104, x_{2*} = 78$, and $x_2^* = 134$. From equation (6.2), we can see that although the system is linear when ρ_k is determined, each coefficient is nonlinear with respect to ρ_k, and the specific value of ρ_k needs to be updated at each sampling time, which reflects the complexity of solving the dynamic optimization problem for the system

First, we compute dynamic optimization problem (6.1) by using the classic PSO algorithm combined with the gradient descent method. The particle position update formula used is as follows: $u_{q,p}^{I_{ter}+1} = u_{q,p}^{I_{ter}} + v_{q,p}^{I_{ter}+1}$. Taking the maximum number of iterations as $I_{ter} = 50$ and the number of particles as $Q = 10$, the results are shown in Figure 1. The upper blue solid line indicates the value of the calculated control quantity, and the lower orange solid line indicates the value of the output y.

Next, we compute the same dynamic optimization problem (6.1) by using the Algorithm 5.1 proposed in this paper and take the same maximum number of iteration steps and number of particles. The results are shown in Figure 2 and Figure 3. As we can see in Figure 3, after

30 iterations, the value function gradually decreases with the number of iteration steps until it stabilizes at a minimum value. Figure 2 shows the value of the fuel control quantity u and the output velocity quantity y at each switching time point. It can be seen from Figure 1 that the control (fuel input) calculated by the classic PSO algorithm appears large fluctuations at many moments, which means that the control (fuel input) is unstable during the actual operation of the engine, which may lead to engine stalling and increase fuel consumption. In contrast, it can be seen from Figure 1 that the control (fuel input) calculated by the MPSO algorithm is relatively much more stable, which is beneficial to the smooth operation of the engine. In addition, the output (speed output of the high-pressure turbine) of the classic PSO algorithm also shows oscillations, implying that the high-pressure rotor speed does not track the target speed well at more momentary points, while the output (speed output of the high-pressure turbine) obtained by the MPSO algorithm is relatively smooth, which implies a better tracking effect. This is mainly because we take into account the actual background of engine acceleration and consider that the fuel control at the previous time would affect the fuel control at the next time. So, the control value at the previous time is added to the formula with a certain weight when updating the particle position. The comparison of numerical results also confirms the effectiveness of our algorithm.

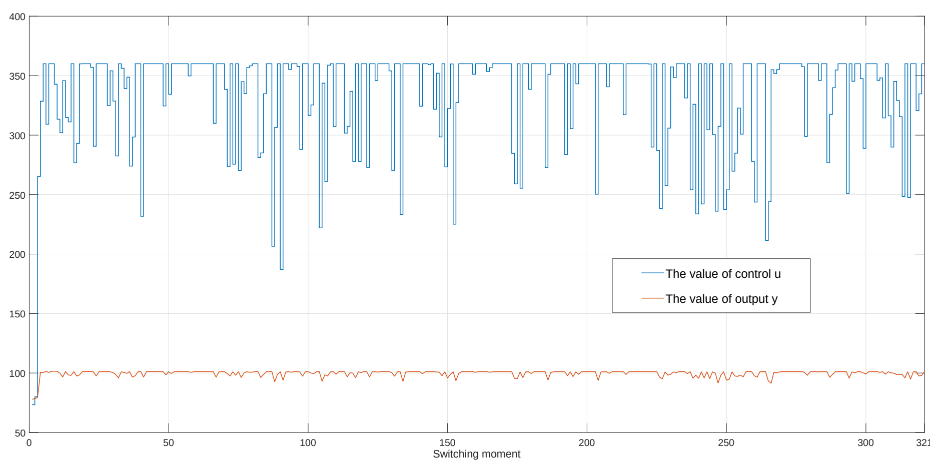

FIGURE 1. The result of the classic PSO algorithm combined with gradient descent

7. CONCLUSION

This paper discussed the dynamic optimization problem of a acceleration process in aero-engine transition state. Relying on the standard control parameterization techniques and the soothing techniques, we propose an optimization algorithm, combined with the gradient descent method and the MPSO algorithm, for solving this problem. The effectiveness of our algorithm is confirmed by numerical calculations and compared with the classic PSO algorithm.

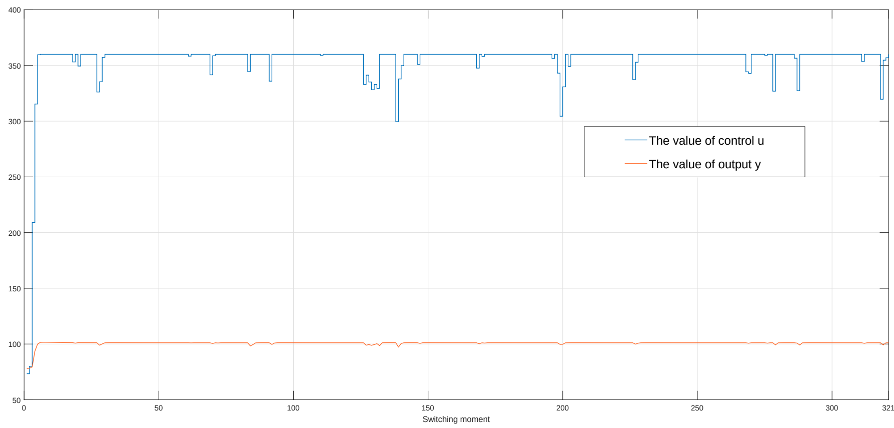

FIGURE 2. The result of the MPSO algorithm combined with gradient descent

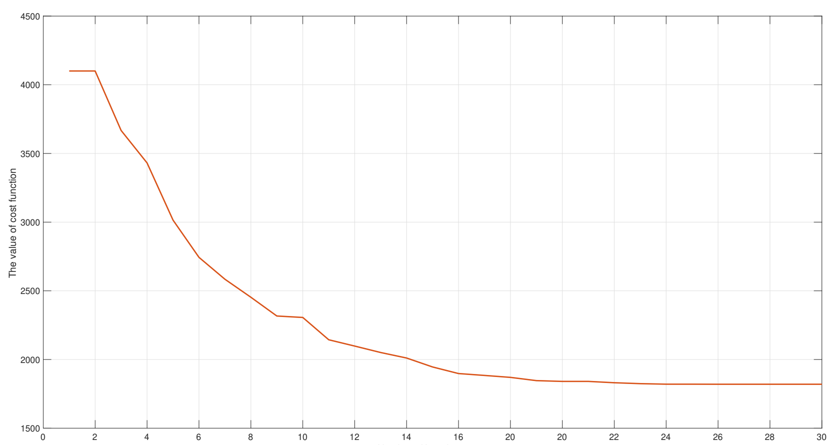

FIGURE 3. Cost function value of the MPSO algorithm combined with gradient descent

Acknowledgments

The second author was supported by the Natural Science Foundation of China (Grant Nos. 11801455, 11871059, and 11971238) and the Open Project of Key Laboratory (Grant No. CSSXKFKTM202004), School of Mathematical Sciences, Chongqing Normal University, China. The third author was supported by the Natural Science Foundation of China (Grant No. 12161076).

REFERENCES

[1] Y. Zhao, J. Zhao, J. Fu, Y. Shi, C. Chen, Rate bumpless transfer control for switched linear systems with stability and its application to aero-engine control design, IEEE Trans. Indust. Electron. 67 (2020), 4900–4910.

[2] C. Chen, J. Zhao, Switching control of acceleration and safety protection for turbo fan aero–engines based on equilibrium manifoldexpansion model, Asian J. Control 20 (2018), 1689–1700.

[3] L.C. Jaw, J.D. Mattingly, Aircraft Engine Controls: Eesign, System Analysis, and Health Monitoring, American Institute of Aeronautics and Astronautics, 2009.

[4] D. Yang, G. Zong, H.R. Karimi, H_∞ refined anti-disturbance control of switched LPV systems with application to aero-engine, IEEE Tran. Indust. Electron. 67 (2020), 3180-3190.
[5] S.Q. Li, S.X. Zhang, Z.Q. Zhou, Improvement of the LPV (linear parameter varying) method for modeling an aeroengine, J. Eng. Thermal Energy Power, 26 (2011), 168-170.
[6] T. Luspay, B. Kulcsár, J.W. Van Wingerden, M. Verhaegen, J. Bokor, Linear Parameter Varying Identification of Freeway Traffic Models, IEEE Trans. Control Sys. Techn. 19 (2011), 31-45.
[7] M. Corno, S.M. Savaresi, G.J. Balas, On linear-parameter-varying (LPV) slip-controller design for two-wheeled vehicles, Int. J. Robust Nonlinear Control, 19 (2009), 1313-1336.
[8] F.D. Bianchi, C. Kunusch, C. Ocampo-Martinez, R.S. Ssnchez-Pena, A gain-scheduled LPV control for oxygen stoichiometry regulation in PEM fuel cell systems, IEEE Trans. Control Sys. Techno. 22 (2014), 1837-1844.
[9] J.M. Biannic, Linear Parameter-Varying Control Strategies for Aerospace Applications. In: Sename O., Gaspar P., Bokor J. (eds) Robust Control and Linear Parameter Varying Approaches. Lecture Notes in Control and Information Sciences, vol 437, pp. 347-373, 2013.
[10] J. Teng, Y. An, L. Wang, Time-optimal control problem for a linear parameter varying system with nonlinear item, J. Franklin Inst. 359 (2022), 859-869.
[11] K. Zhu, J. Zhao, G.M. Dimirovski, H_∞ tracking control for switched LPV systems with an application to aero-engines, IEEE/CAA J. Automatica Sinica, 5 (2018), 699-705.
[12] D. Yang, J. Zhao, H_∞ output tracking control for a class of switched LPV systems and its application to an aero-engine model, Int. J. Robust & Nonlinear Control 27 (2017), 2102-2120.
[13] J. Zhai, T. Niu, J. Ye, E. Feng, Optimal control of nonlinear switched system with mixed constraints and its parallel optimization algorithm, Nonlinear Anal. 25 (2017), 21–40.
[14] A.B. Hempel, P.J. Goulart, J. Lygeros, Strong stationarity conditions for optimal control of hybrid systems, IEEE Trans. Auto. Control 62 (2017), 4512–4526.
[15] S.Y. Lv, R. Tao, Z. Wu, Maximum principle for optimal control of anticipated forward-backward stochastic differential delayed systems with regime switching, Optim. Control Appl. Methods 37 (2016), 154–175.
[16] M. Chambers, The mathematical theory of optimal processes, J. Oper. Res. Soc. 16 (1965), 493–494.
[17] J. Yuan, L. Wang, J. Xie, K.L. Te, Optimal minimal variation control with quality constraint for fed-batch fermentation processes involving multiple feeds, J. Franklin Inst. 357 (2020), 6571-6594.
[18] A.I. Selvakumar, K. Thanushkodi, A new particle swarm optimization solution to nonconvex economic dispatch problems, IEEE Trans. Power Sys. 22 (2007), 42-51.
[19] R.J. Kuo, C.M. Chao, Y.T. Chiu, Application of particle swarm optimization to association rule mining, Appl. Soft Computing 11 (2011), 326-336.
[20] R.C. Loxton, K.L. Teo, V. Rehbock, W.K. Ling, Optimal switching instants for a switched-capacitor DC/DC power converter, Automatica, 45 (2009), 973-980.
[21] R.C. Loxton, K.L. Teo, V. Rehbock, Computational method for a class of switched system optimal control problems, IEEE Trans. Auto. Control, 54 (2009), 2455-2460.
[22] N.U. Ahmed, Elements of Finite-Dimensional Systems and Control Theory, Essex: Longman Scientific and Technical, 1988.
[23] J. Kennedy, R.C. Eberhart, Particle swarm optimization, Proceeding of the IEEE Int'l Conference on Neural Networks. Perth Australia, IEEE Press, 1995.
[24] R.C. Loxton, Optimal control problems involving constrained, switched, and delay systems, Curtin University, 2010.
[25] R. Loxton, Q. Lin, V. Rehbock, K.L. Teo, Control parameterization for optimal control problems with continuous inequality constraints: New convergence results, Numer. Algebra, Control Optim. 2 (2012), 571-599.
[26] C.J. Goh, K.L. Teo, Control parametrization: a unified approach to optimal control problems with general constraints, Automatica 24 (1988), 3-18.